Molecular Therapy
Oncolytics
Original Article

AMERICAN SOCIETY of GENE & CELL THERAPY

Optimization of a Neural Stem-Cell-Mediated Carboxylesterase/Irinotecan Gene Therapy for Metastatic Neuroblastoma

Margarita Gutova,[1] Leanne Goldstein,[2] Marianne Metz,[1] Anahit Hovsepyan,[3,4] Lyudmila G. Tsurkan,[5] Revathiswari Tirughana,[1] Lusine Tsaturyan,[1] Alexander J. Annala,[1] Timothy W. Synold,[6] Zesheng Wan,[7] Robert Seeger,[7] Clarke Anderson,[8] Rex A. Moats,[3,4] Philip M. Potter,[5] and Karen S. Aboody[1]

[1]Departments of Developmental and Stem Cell Biology, City of Hope National Medical Center and Beckman Research Institute of City of Hope, Duarte, CA 91010, USA; [2]Information Sciences, City of Hope National Medical Center and Beckman Research Institute of City of Hope, Duarte, CA 91010, USA; [3]Departments of Radiology and Pathology, Keck School of Medicine, University of Southern California, Los Angeles, CA 90033, USA; [4]Department of Biomedical Engineering, Viterbi School of Engineering, University of Southern California, Los Angeles, CA 90089, USA; [5]Department of Chemical Biology & Therapeutics, St. Jude Children's Research Hospital, Memphis, TN 38101, USA; [6]Department of Cancer Biology, City of Hope National Medical Center and Beckman Research Institute of City of Hope, Duarte, CA 91010, USA; [7]Children's Center for Cancer and Blood Diseases, CHLA/Keck School of Medicine, University of Southern California, Los Angeles, CA 90033, USA; [8]Department of Pediatric Oncology, City of Hope National Medical Center and Beckman Research Institute of City of Hope, Duarte, CA 91010, USA

Despite improved survival for children with newly diagnosed neuroblastoma (NB), recurrent disease is a significant problem, with treatment options limited by anti-tumor efficacy, patient drug tolerance, and cumulative toxicity. We previously demonstrated that neural stem cells (NSCs) expressing a modified rabbit carboxylesterase (rCE) can distribute to metastatic NB tumor foci in multiple organs in mice and convert the prodrug irinotecan (CPT-11) to the 1,000-fold more toxic topoisomerase-1 inhibitor SN-38, resulting in significant therapeutic efficacy. We sought to extend these studies by using a clinically relevant NSC line expressing a modified human CE (hCE1m6-NSCs) to establish proof of concept and identify an intravenous dose and treatment schedule that gave maximal efficacy. Human-derived NB cell lines were significantly more sensitive to treatment with hCE1m6-NSCs and irinotecan as compared with drug alone. This was supported by pharmacokinetic studies in subcutaneous NB mouse models demonstrating tumor-specific conversion of irinotecan to SN-38. Furthermore, NB-bearing mice that received repeat treatment with intravenous hCE1m6-NSCs and irinotecan showed significantly lower tumor burden (1.4-fold, $p = 0.0093$) and increased long-term survival compared with mice treated with drug alone. These studies support the continued development of NSC-mediated gene therapy for improved clinical outcome in NB patients.

INTRODUCTION

Neuroblastoma (NB) is a neuroendocrine tumor that arises from neural crest elements of the sympathetic nervous system. It is the most common extracranial solid tumor of childhood, with a long-term survival rate of only 15%.[1] Nearly all of the 45% of NB patients diagnosed with high-risk tumors present with metastases, including those diagnosed at any age with amplification of the *MYCN* oncogene and those older than 18 months with non-*MYCN*-amplified tumors.[2–5] Although patient outcomes have steadily improved over the past 20 years, 3-year event-free survival rate is only 40% for patients who have high-risk, stage 4 metastatic disease.[6] The current standard of care for these patients consists of: (1) intensive induction chemotherapy, (2) myeloablative consolidation chemoradiotherapy and autologous hematopoietic stem cell transplantation, and (3) 13-*cis* retinoic acid with immunotherapy that targets disialoganglioside (GD2).[6–9] Treatment failures occur at both primary and metastatic sites, and particularly in metastases to the bone and bone marrow, suggesting that minimal residual disease is an important cause of recurrence.[6] Current regimens of dose-intensive chemotherapy and irradiation are likely at the limit of both anti-tumor efficacy and patient tolerance, and post-consolidation therapy does not eradicate minimal residual disease (MRD) in many patients.[6–9] Therefore, there is a critical need for improved, less toxic therapeutic approaches for tumor cyto-reduction (induction and consolidation phases) and eradication of MRD (post-consolidation phase) to improve clinical outcome in children with this disease.

Selective activation of the prodrug irinotecan (CPT-11; Camptosar; 7-ethyl-10-[4-(1-piperidino)-1-piperidino]carbonyloxycamptothecin) to its 1,000-fold more cytotoxic active metabolite SN-38 (7-ethyl-10-hydroxycamptothecin), a topoisomerase-1 inhibitor, can be achieved with carboxylesterases (CEs). This activation results in increased cytotoxicity and improved antitumor response in human tumor xenograft models of NB.[10] Irinotecan is currently being used in

Received 29 November 2016; accepted 29 November 2016;
http://dx.doi.org/10.1016/j.omto.2016.11.004.

Correspondence: Karen S. Aboody, Department of Developmental and Stem Cell Biology, City of Hope National Medical Center and Beckman Research Institute, 1500 E. Duarte Road, Duarte, CA 91010, USA.
E-mail: kaboody@coh.org

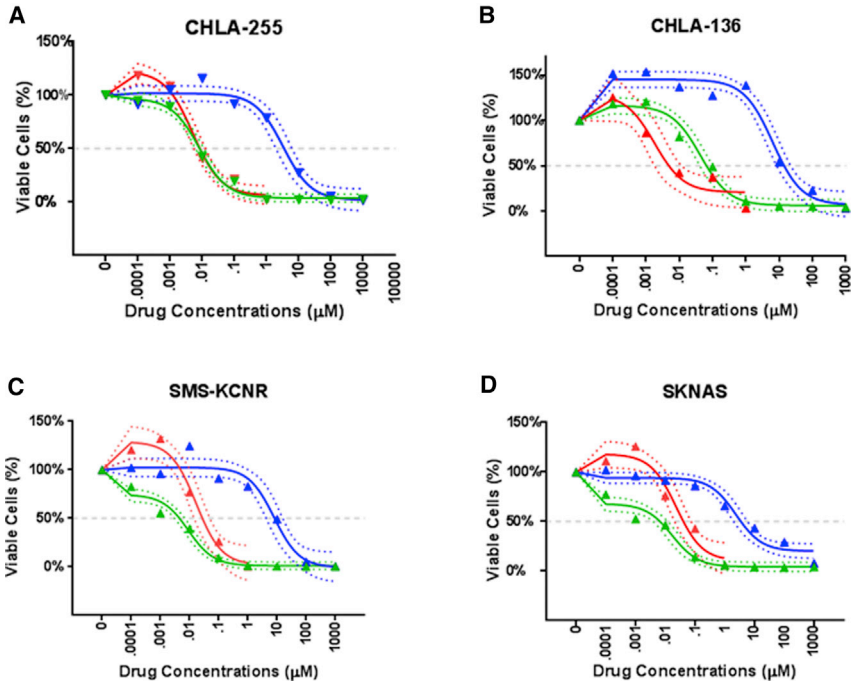

Figure 1. Half-Maximal Inhibitory Drug Concentrations of Irinotecan and SN-38 for Human NB Cell Lines

IC_{50} estimates and confidence intervals were estimated using the One Site–Fit Log IC_{50} non-linear function in GraphPad Prism using all concentrations larger than baseline. Baseline values were excluded because they offset the function, slightly biasing estimates. Shown are graphs of cell viability by drug concentration for the human NB cell lines (A) CHLA-255, (B) CHLA-136, (C) SMS-KCNR, and (D) SKNAS. Drug treatments were irinotecan alone (blue), SN-38 alone (red), and hCE1m6-NSC CM + irinotecan (green). Three independent experiments were performed in triplicates. Triangles indicate mean observed values, solid lines are estimates from Prism function, and dotted lines are 95% confidence bands.

front-line treatment for NB and tested in combination with other drugs in a phase I clinical trial for this disease,[11] as well as colon cancer.[12,13] Clinical trials with this agent are also under way in variety of other solid malignancies (e.g., sarcomas and non-small-cell lung cancer).[14–18]

Neural stem cells (NSCs) are inherently tumor tropic and selectively localize to solid tumor foci in multiple organs after intravenous administration in several metastatic tumor models, including breast cancer,[19–21] ovarian cancer,[22] lung cancer,[23] and NB.[24–26] NSC-mediated enzyme and prodrug therapy has been shown to be effective in several tumor models including glioma, medulloblastoma, melanoma brain metastases, and metastatic breast cancer.[19,27–29] We previously showed proof of concept for increased therapeutic efficacy in mouse models of metastatic NB, using tumor-tropic NSCs expressing a modified rabbit carboxylesterase (rCE) to convert the prodrug irinotecan to SN-38.[10,19,30] We now present data using a well-characterized, clonal human NSC line (HB1.F3.CD clone 21)[27] that has demonstrated clinical safety and proof of concept for brain tumor localized, NSC-expressed enzyme-mediated conversion of a prodrug (5-fluocytosine) to its active chemotherapeutic (5-fluorouracil) (investigational new drug [IND] application 14041; NCT01172964).[31] We transduced this NSC line with replication-deficient adenovirus designed to allow high-level, transient expression and secretion of a modified human CE1 (hCE1m6). The hCE1m6-expression vector was generated from the human liver CE hCE1, specifically to allow for efficient conversion of irinotecan to SN-38,[32] and has demonstrated functional equivalence to rCE, both in vitro and in vivo.[33] This NSC-secreted form of CE accumulates at tumor foci (because of NSC tropism to tumor sites), where it can convert administered irinotecan to SN-38 and can generate a greater therapeutic radius of tumor kill around each NSC (the "bystander effect"), as compared with irinotecan alone.[34,35] Toward clinical translation, our goal was to maximize therapeutic efficacy by determining the optimal clinically relevant dose and schedule of hCE1m6-NSCs + irinotecan in a mouse model of metastatic NB. Repeat treatment of mice bearing NB with intravenously administered hCE1m6-NSCs and irinotecan resulted in both a significant decrease in tumor burden (1.4-fold, $p = 0.0093$) and increased long-term survival versus treatment with irinotecan alone. These studies support further development of NSC-mediated gene therapy for improved clinical outcome in NB patients.

RESULTS

In Vitro Sensitivity of Human NB Cell Lines to Irinotecan and SN-38

To determine whether hCE1m6 expressed by NSCs could enhance the cell-killing effects of irinotecan on NB cells, we measured the half-maximal inhibitory drug concentration (IC_{50}) for the drug in the presence and absence of NSC-secreted hCE1m6. The cytotoxicity of irinotecan and SN-38 was determined for a panel of human-derived NB cell lines (SMS-KCNR, CHLA-255, CHLA-136, and SK-N-AS) (Figure 1; Table 1). In brief, NB cells were incubated for 4 hr in cell culture medium containing irinotecan (0.001–1,000 μM) or SN-38 (1–100 nM), or in conditioned media (CM) harvested from NSCs expressing hCE1m6 to which irinotecan (1–100 μM) was added. All NB cell lines were significantly more sensitive to irinotecan in the presence of hCE1m6 as compared with irinotecan alone (Figures 1A–1D) (Table 1), because of conversion of irinotecan to SN-38, as demonstrated before.[33] For the most sensitive cell line, SMS-KCNR, the cytotoxicity of irinotecan ($IC_{50} = 7.95$ μM) was increased up to ~900-fold by addition of hCE1m6-NSC CM ($IC_{50} = 0.009$ μM). Although the change in sensitivity was not as dramatic in the other cell lines, addition of hCE1m6-NSC CM led to an increase of at least 139-fold (Table 1). These data suggest that

Table 1. IC_{50} Values for NB Cell Lines Treated with Irinotecan, hCE1m6 + Irinotecan, or SN-38

NB Cell Line	IC_{50} Values (μM) (95% Confidence Interval)			Fold Decrease in IC_{50}, as Compared with Irinotecan
	Irinotecan	SN-38	hCE1m6 + Irinotecan	
CHLA-255	3.29 (1.56, 6.83)	0.005 (0.003, 0.009)	0.008 (0.006, 0.012)	411
CHLA-136	6.41 (3.51, 11.71)	0.002 (0.0004, 0.007)	0.043 (0.025, 0.075)	149
SMS-KCNR	7.95 (3.36, 18.83)	0.017 (0.007, 0.041)	0.009 (0.005, 0.015)	883
SKNAS	2.36 (1.20, 4.64)	0.024 (0.009, 0.059)	0.017 (0.008, 0.034)	139

hCE1m6 produced by NSCs can effectively convert irinotecan to the active metabolite SN-38, reaching therapeutic IC_{50} levels similar to those observed for SN-38 alone. Important for clinical translation, only nanomolar levels of SN-38 are needed for significant efficacy (Table 1).

NSC Clearance from Circulation and Peripheral Organs in Non-Tumor-Bearing Mice

Before translating use of hCE1m6-NSCs to a therapeutic approach, it will be necessary to ensure that these cells do not localize to non-tumor-harboring tissues and organs. To assess this, we performed in vivo time-dependent NSC biodistribution or clearance studies. For all experiments, plasma-esterase-deficient mice (*Es1*^{e}/SCID)[36] were used to more closely represent human plasma esterase levels. This allows for assessment of clinically relevant human doses of irinotecan in these mice.

Because the hCE1m6-NSCs have a single copy of the v-*myc* gene per cell,[27] we used qPCR (TaqMan qPCR) to quantify the relative amounts of NSCs in the circulation and major organs. One hour after intravenous administration into non-tumor-bearing *Es1*^{e}/SCID mice,[36] NSCs were detected in the lungs, liver, spleen, blood, and brain (Figure 2A). However, hCE1m6-NSCs were undetectable by PCR at 24 hr, 48 hr, and 5 days post-injection (Figure 2A, 1 and 24 hr time points are shown). At the 1 hr time point, the relative rank of v-*myc*-positive cells per 100,000 normal tissue cells was lung > blood > liver > spleen > brain. Statistically significant differences were found when numbers of NSCs in lung were compared with blood ($p = 0.02$), liver ($p = 0.003$), spleen ($p = 0.003$), and brain ($p = 0.007$), because it is likely that the majority of stem cells are initially trapped in the lungs.[37] No detectable v-*myc* DNA was observed 24 hr after NSC injection, indicating essentially total clearance of NSCs by this time point. Brain, liver, lung, and kidneys harvested at 1 and 24 hr after NSC administration were further analyzed by Prussian blue staining and histological examination to detect iron-labeled hCE1m6-NSCs (positive control for Prussian blue staining of Molday iron-labeled hCE1m6-NSCs was subcutaneous SKNAS tumor sections with NSCs; data not shown). We did not see any cells that were positive for Prussian blue staining in any of the sample tissue sections examined (Figure 2B), indicating the retention of exogenous hCE1m6-NSCs in normal tissues is a rare event and, given the assays used, detectable only by qPCR.

Biodistribution of Intravenously Administered NSCs to Subcutaneous NB Tumors

To confirm that hCE1m6-NSCs could localize to NB tumors, we developed subcutaneous xenografts of all four human NB cell lines in *Es1*^{e}/SCID mice. When tumors became palpable, mice were intravenously injected with 2×10^6 hCE1m6-NSCs. Forty-eight hours later, tumors were excised and analyzed for the presence of cells containing v-*myc*. All NB tumors contained NSCs (Figure 3). The average NSC tumor distributions for CHLA-136, SMS-KCNR, CHLA-255, and SK-N-AS NB xenografts were 269 ± 340, 153 ± 312, 124 ± 223, and 38 ± 27 NSCs per 100,000 tumor cells, respectively. The levels of v-*myc* among the samples, both within the same tumor samples or among mouse tumors, were highly variable, and averages were not significantly different (as assessed by analysis of variance). This was similar to previous observations for which NSC distribution was heterogeneous in other solid tumor models.[27,30]

Kinetics of hCE1m6-NSC-Mediated Conversion of Irinotecan to SN-38 in Subcutaneous NB Tumors

Following establishment of subcutaneous CHLA-255 or CHLA-136 NB xenografts in *Es1*^{e}/SCID mice, we intravenously injected tumor-bearing mice with 2×10^6 hCE1m6-NSCs on day 0 and with irinotecan (15 mg/kg) on day 2. One hour after drug administration, mice were sacrificed and NB tumors were excised and analyzed for drug (irinotecan and SN-38) levels by high-performance liquid chromatography-MS/MS. SN-38 levels in both CHLA-255 and CHLA-136 NB tumors in mice that received hCE1m6-NSCs were highest when irinotecan was given 2 days after NSC administration (Figure 4). We saw an approximately 2-fold increase in SN-38 concentrations in tumors from mice that received hCE1m6-NSCs on day 2 after NSC injection versus treatment with irinotecan alone (CHLA-255: 445.1 ± 69.0 versus 217.7 ± 60.7 ng/mL [2.0-fold difference, $p = 0.0001$]; CHLA-136: 766.7 ± 154.1 versus 460.9 ± 87.1 ng/mL [1.7-fold difference, $p = 0.0069$). In contrast, plasma concentrations of SN-38 were similar in all mice, regardless of whether they received hCE1m6-NSCs. No significant differences in SN-38 concentrations were observed at 3 or 4 days after hCE1m6-NSC injection as compared with irinotecan alone in all mice (data not shown).

Therapeutic Efficacy of hCE1m6-NSCs and Irinotecan in a Metastatic NB Model

To assess the efficacy of treatment of hCE1m6 NSCs and irinotecan, we intravenously injected 2×10^6 CHLA-136 NB cells expressing

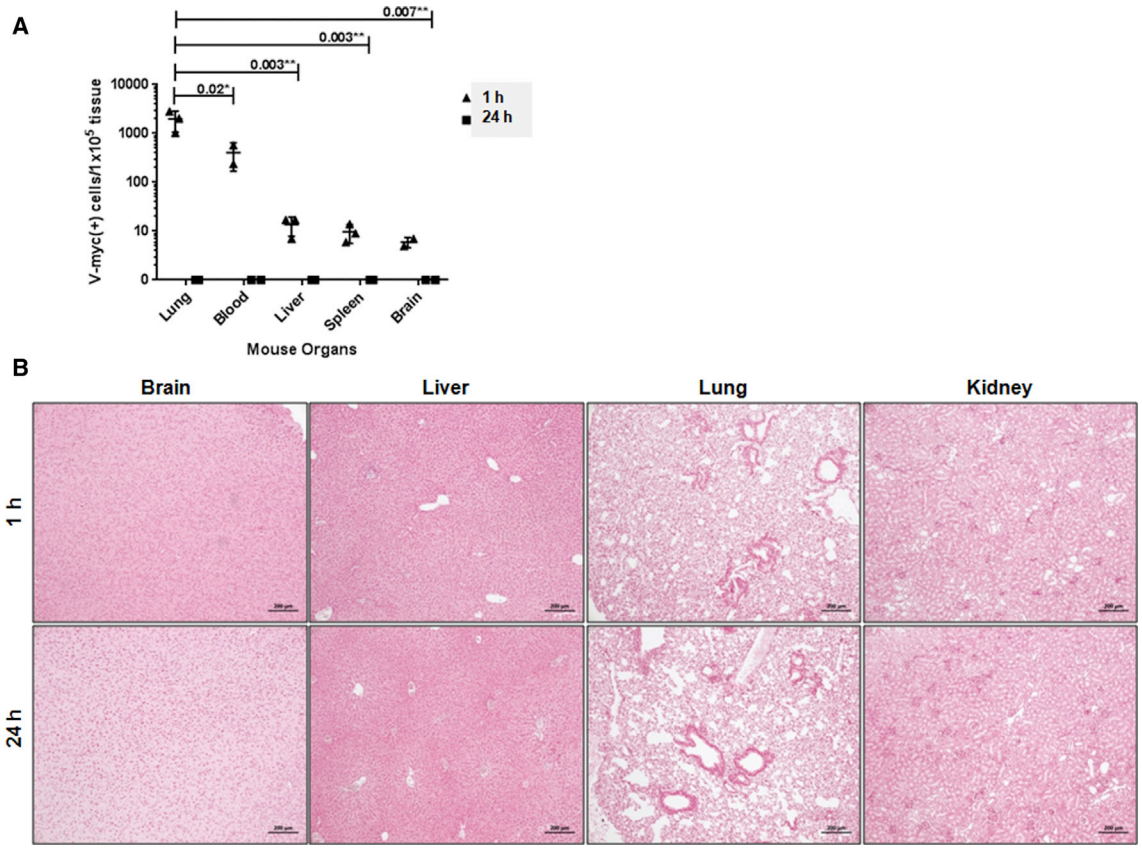

Figure 2. Clearance of hCE1m6-NSC from Peripheral Organs in Non-Tumor-Bearing *Es1*^{e}-Deficient Mice

(A) qPCR analysis of v-*myc* transcripts in lung, blood, liver, spleen, and brain of non-tumor-bearing mice. (B) Prussian blue-stained peripheral mouse organs 1 and 24 hr after hCE1m6-NSC administration. Scale bars, 200 μm.

firefly luciferase Ffluc into *Es1*^{e}/SCID mice on day 0, and treatment was initiated on day 10. Tumor growth was monitored by bioluminescent imaging, and mean signal intensities were obtained from these scans at multiple times points for each mouse. Two days after intravenous administration of hCE1m6-NSCs, mice were treated with three rounds of irinotecan using an established clinical dosing regimen.[38] Treatment groups included: group A, tumor only; group B, irinotecan only (7.5 mg/kg, three times a week); group C, hCE1m6-NSCs + irinotecan (7.5 mg/kg, three times a week); group D, irinotecan only (15 mg/kg, three times a week); and group E, hCE1m6-NSCs + irinotecan at (15 mg/kg, three times a week). Two weeks of treatment was followed by 1 week of rest (considered one cycle of therapy). The treatment cycle was repeated three to four times. Mice that received hCE1m6-NSCs in combination with irinotecan (15 mg/kg, approximately equivalent to human dose of 50 mg/m^2), demonstrated a significant delay in tumor growth as compared with those that received irinotecan alone (Figure 5A), resulting in a 1.7-fold log scale decrease in luciferase signal intensity at day 88 ($p = 0.0001$). We saw no difference in tumor growth between mice that did or did not receive NSCs when 7.5 mg/kg irinotecan was used. The observed delay in tumor growth was associated with a significant extension of median survival in mice treated with hCE1m6-NSCs and irinotecan (15 mg/kg) (137 days; 95% confidence interval [CI], 126–139 days) versus drug alone (117 days; 95% CI, 112–126 days; $p = 0.034$) (Figure 5B). Similar studies using the CHLA-255 tumor line also demonstrated a significant delay in tumor growth in mice treated with hCE1m6-NSCs and irinotecan (15 mg/kg) treatment versus drug alone (0.74-fold decrease in tumor growth at day 42, $p = 0.0080$).

To further analyze the effect of this NSC-mediated gene therapy, we histologically examined whether metastatic foci were present in the liver, lungs, and kidneys (Figure 6). Mice treated with hCE1m6-NSCs and irinotecan (15 mg/kg) in group E showed a significant reduction in tumor burden in the liver, with only two of eight animals demonstrating tumors in this organ as compared with all (8/8) control mice (no treatment, tumor only; $p = 0.0070$) (Figure 6; Table 2). We also saw fewer tumor foci in the irinotecan alone (15 mg/kg) treatment group (5/7); however, this result was not significant ($p = 0.31$; Table 2). NB lesions were infrequently seen in the lungs of untreated mice (3/8), and none was observed in mice that underwent high-dose (15 mg/kg) irinotecan alone therapy. No differences were seen in the presence of tumors in the kidney in any of the cohorts (Table 2).

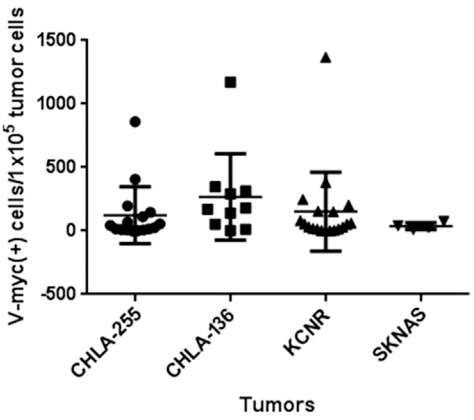

Figure 3. qPCR Analysis of Numbers of hCE1m6-NSCs at Subcutaneous NB Tumors

Note that each NSC has one copy of the v-*myc* gene.

DISCUSSION

The data presented here support further efforts toward clinical translation studies of this CE-irinotecan enzyme-prodrug gene therapy approach for high-risk NB patients using an NSC line that has demonstrated clinical safety in brain tumor patients (NCT01172964). These cells have been transduced ex vivo with an adenovirus designed to express a modified human CE (hCE1m6), an enzyme highly proficient at irinotecan activation. Ex vivo transduction of NSCs with replication-deficient adenovirus offers several advantages, including: (1) high, transient secretion of hCE1m6, providing an expanded radius of action via the enzyme-prodrug bystander effect[34,35]; (2) non-integration into the DNA of the parent NSC line, avoiding the possibility of insertional mutagenesis; and (3) the potential to increase the effectiveness of a clinically approved chemotherapeutic agent by significantly increasing intratumoral concentrations of the active drug.

Treatment of several human-derived NB lines with media harvested from NSCs secreting hCE1m6 and irinotecan demonstrated 139- to 883-fold lower IC_{50} values when compared with treatment with drug alone. This is consistent with the enhanced hydrolysis of irinotecan in the media, resulting in significantly higher concentrations of SN-38, leading to increased cytotoxicity. Because only nanomolar levels of SN-38 are needed for tumor cytotoxicity, increased drug activation at tumor foci using NSCs can be achieved using this strategy.

In vivo studies in *Es1*^{e}/SCID mice demonstrated that hCE1m6-NSCs are cleared from normal organs within 24 hr of intravenous administration. This is an advantage over mesenchymal stem cells (MSCs), which are larger and can get trapped in the lungs.[37] Because clearance of NSCs from normal tissues will be important for limiting off-target effects, based on these results, we decided to wait at least 2 days after NSC administration before treating with irinotecan in in vivo studies. We also confirmed (by qPCR for v-*myc*) that hCE1m6-NSCs selectively localize to NB tumors, although v-*myc* expression among the samples, both within the same tumor and between tumors, was highly variable. This finding is consistent with other results showing heterogeneous NSC distribution within metastatic tumor foci in other metastatic solid tumor models.[27,28,39] Additional studies that may enhance NSC-tumor tropism would allow for further optimization, but this would require a detailed understanding of the mechanism by which these cells target tumors in vivo.[39] Because such information is currently lacking, efforts to further improve NSC-directed tumor targeting will likely require further studies to dissect the homing and signaling cascades in this process. Such studies are currently under way. However, it is possible that administering the NSCs in multiple doses (such as two to four times in one day) rather than as a single bolus dose may improve biodistribution within and among tumor foci. Again, detailed preclinical studies will be necessary to validate this hypothesis.

In vivo pharmacokinetic studies indicated that the optimal timing for irinotecan administration was 2 days after hCE1m6-NSCs. In these experiments, approximately 2-fold higher SN-38 concentrations were seen in the presence of hCE1m6-NSCs on day 2 versus irinotecan treatment alone. No significant increase in SN-38 levels were observed at days 3 and 4 (as compared with non-NSC-injected animals), and the exact reasons for this are unclear. It may result from reduced expression of hCE1m6 from the NSCs in vivo, diffusion of the secreted CE away from the tumor xenografts, and/or enhanced proteolysis of the secreted enzyme. However, based upon these results, therapeutic efficacy studies were conducted in NB metastatic models, using clinically relevant concentrations of irinotecan given 2 days post-NSC administration. This resulted in significantly delayed progression of

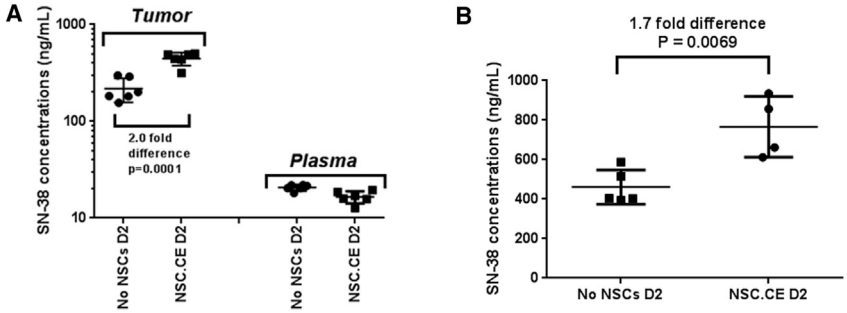

Figure 4. Kinetics of CE-Mediated Conversion of Irinotecan to SN-38 in Subcutaneous NB Tumors, CHLA-255 and CHLA-136

(A) SN-38 concentrations in CHLA-255 tumors and plasma from mice treated with intravenously administered hCE1m6-NSCs on day 0, and 2 days later with intravenous irinotecan. Mice were euthanized and tumors collected 1 hr after irinotecan administration. Data shown are mean ± SD (n = 6). (B) SN-38 concentrations in CHLA-136 tumors from mice treated as described in (A).

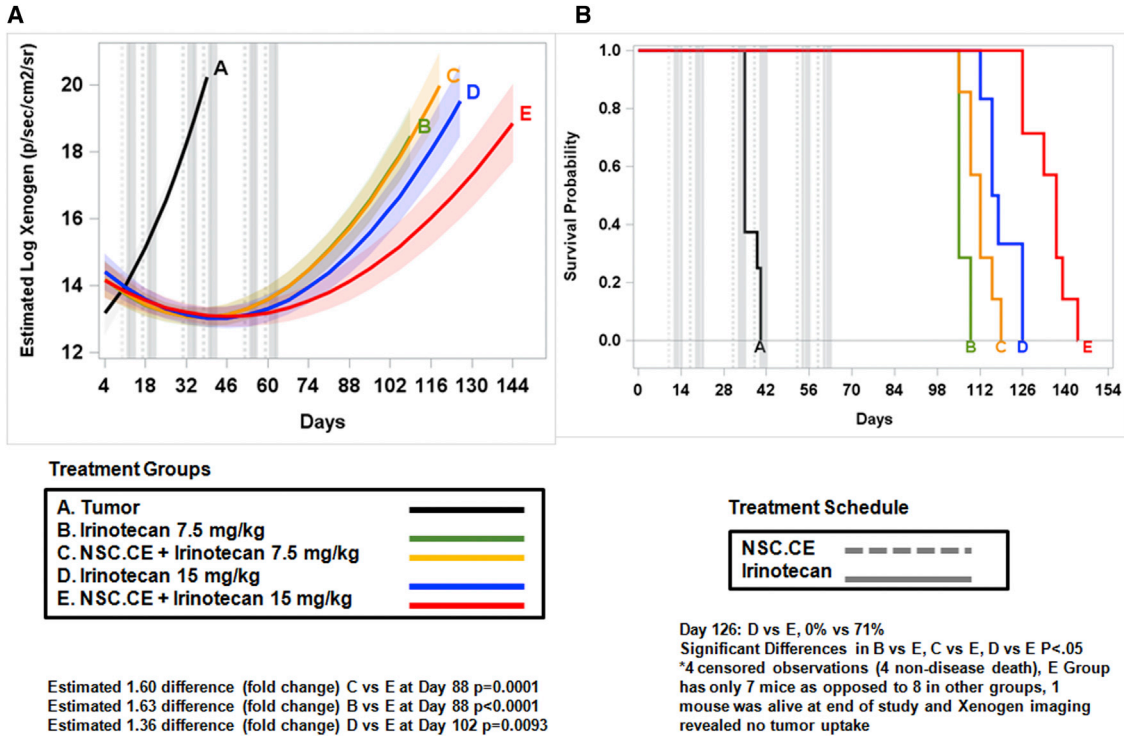

Figure 5. Therapeutic Efficacy of Treatment with hCE1m6-NSCs and Irinotecan in CHLA-136 NB Metastatic Mouse Model

(A) Model estimated log-transformed Xenogen signal over days by treatment group. Gray vertical dashed and solid lines indicate when NSC and irinotecan treatments were administered. Light shading around each treatment group line indicates 95% confidence interval bands around estimates. (B) Kaplan-Meier survival curves by treatment group. Gray vertical dashed and solid lines indicate when NSC and irinotecan treatments were administered. Each cycle was 2 weeks on, 1 week off. Treatment regimen includes three cycles.

tumor growth in mice that received hCE1m6-NSCs in combination with the drug (15 mg/kg). In addition, there was a significant delay in tumor growth in these mice as compared with animals that received irinotecan alone. Although this establishes proof of concept for this approach, further studies are warranted to optimize the conditions for maximal therapeutic efficacy. For example, cell dosing strategies that lead to an increase in both the number and the coverage of NSCs in tumors would be expected to result in even greater intratumoral conversion of the irinotecan to SN-38 and may further prolong survival. Furthermore, increasing tumor biodistribution of NSCs by fractionating the dose of cells may further prolong survival. This is based on the pattern observed of the log Xenogen signal.

Finally, mice treated with hCE1m6-NSCs and irinotecan (15 mg/kg) demonstrated significantly less tumor burden in the liver as compared with control animals (6/8 had no tumor). Minimizing liver metastases clinically may help preserve hepatic function. leading to improved quality of life and toleration of hepatically metabolized drugs. Interestingly, mice with liver tumors in the irinotecan-treated groups (either with or without hCE1m6-NSCs) had fewer large, consolidated tumors, as compared with higher numbers of small tumors distributed throughout this organ in control animals. Additional studies are currently ongoing in other mouse models of liver metastases to determine whether there is an organ-site-specific effect of the NSCs, and if so, what the mechanism of this effect might be.

Collectively, the studies described herein demonstrate that hCE1m6-NSCs can increase SN-38 levels at tumor sites as compared with irinotecan treatment alone and have a marked effect on NB progression. In the future, the addition of temozolomide may further enhance the activity of treatment with hCE1m6-NSCs plus irinotecan by creating topoisomerase 1-DNA complexes that may augment the activity of irinotecan. This should lead to enhanced antitumor activity. Furthermore, patients with other cancers that are often treated with irinotecan, such as metastatic colon cancer that involves the liver, may also benefit from this therapy. As a consequence, further studies that seek to develop this NSC-mediated gene therapy strategy are in progress for facile translation to the clinic.

MATERIALS AND METHODS

Cell Culture and Cytotoxicity Assays

NB Tumor Cells

CHLA-255, CHLA-136, and SMS-KCNR human NB lines were transduced with the firefly luciferase (Fluc) gene using a lentivirus vector.[40] CHLA-255-Fluc and CHLA-136-Fluc were cultured in Iscove's modified Dulbecco's medium (IMDM) supplemented with 10% fetal

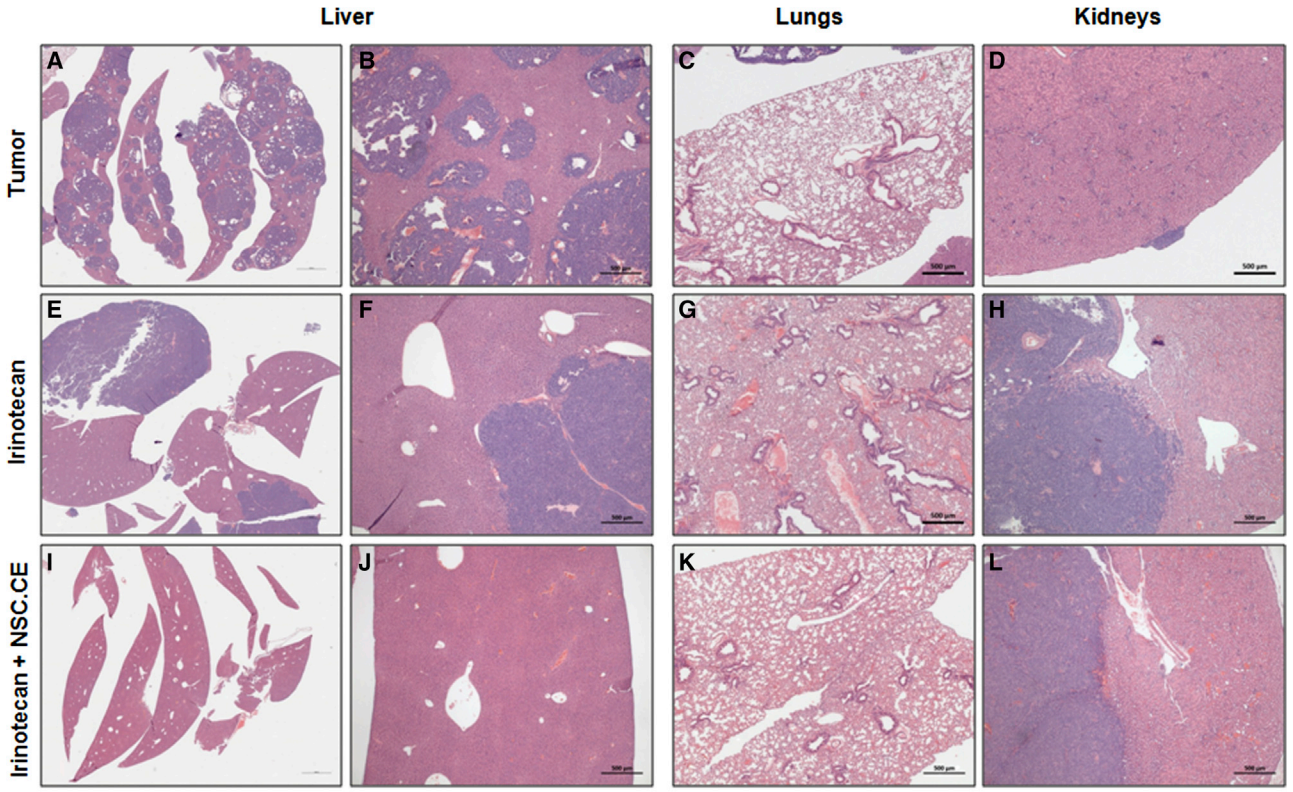

Figure 6. Histological Analysis of Organs from Mice Treated with hCE1m6-NSCs and Irinotecan

(A–D) Controls (tumor) were organs from untreated mice. (E–L) H&E-stained tissue sections from peripheral mouse organs (liver, lung, and kidney) after treatment with three cycles of irinotecan alone (E–H) or irinotecan/hCE1m6-NSC therapy (2 weeks on 1 week off) (I–L). Scale bars, 500 μm.

bovine serum (FBS), 1% L-glutamine (100×, 25030-164; GIBCO) and 1% penicillin-streptomycin (catalog no. 15140; GIBCO). SMS-KCNR-Fluc cells were cultured in RPMI 1640 supplemented with 10% FBS, 1% L-glutamine (100×, catalog no. 25030-164; GIBCO) and 1% penicillin-streptomycin (catalog no. 15140; GIBCO). For cytotoxicity assays, NB cells were seeded into each well of 96-well white opaque culture plates (catalog no. 353296; Falcon/Corning) and grown overnight (CHLA-255-Fluc, 4E3 cells/well; CHLA-136-Fluc, 5E3 cells/well) or for 3 days (SMS-KCNR-Fluc, 1E4 cells/well). NB cells were then exposed for 4 hr to: (1) SN-38 (0.001–1 nM) in cell culture media, (2) irinotecan (0.001–1,000 μM) in cell culture media, or 3) irinotecan (0.001–1000 nM) in conditioned media from hCE1m6-NSCs. The media were then replaced with fresh culture media and cells were incubated for 5 days. Beetle luciferin (5 mg/mL; catalog no. E1605; Promega) was then added to each well, and cells were incubated for 5 min in the dark, after which cell viability was measured as Ffluc luminescence using a GloMax Multi-Detection System (model E8032; Promega).

Statistical Analyses

Statistical analyses were performed using SAS (Statistical Analysis System) version 9.4 and Prism version 6. Cell viability was measured in triplicate at each concentration. Values for each cell line were normalized relative to average baseline (no drug control) viability. IC_{50} values were estimated with 95% confidence intervals using the One Site–Fit Log IC_{50} non-linear function in Prism 6. Statistical significance at an alpha level of 0.05 was ascertained by non-overlapping confidence intervals. Graphs of functions were produced using Prism 6. Baseline measurements were excluded from analyses because they offset the function.

Neural Stem Cells

All in vivo and in vitro studies used a clonal v-*myc* immortalized human NSC line, HB1.F3.CD clone 21 (HB1.F3.CD21; established as a Master Cell Bank [MCB] at passage 20 at the City of Hope). NSCs from the MCB were thawed and expanded in T-175 tissue culture flasks in DMEM (10313-021; Invitrogen) supplemented with 10% heat-inactivated FBS (SH30070.03; HyClone) and 2 mM L-glutamine (25030-081; Invitrogen) as described previously.[41] NSCs were then transduced overnight with a clinical-grade recombinant replication-deficient adenovirus encoding hCE1m6 (AdV.hCE1m6),[27] resulting in transient secretion hCE1m6.[32]

In Vivo hCE1m6-NSC Studies

NSC Clearance Studies in Non-Tumor-Bearing Mice

All mouse studies were conducted under a City of Hope Institutional Animal Care and Use Committee (IACUC)-approved protocol

Table 2. Summary of Histological Analysis of Peripheral Mouse Organs after Three Cycles of Therapy: CHLA-136 Tumor Model

Metastasis	Mice per Group	Kidney	Liver (No. of Foci)	Lungs
Group A	8	5/8	8/8 (>20)	3/8
Group B	8	6/8	6/8 (<10)	2/8
Group C	8	7/8	6/8 (<10)	1/8
Group D	7	5/7	5/7 (<5)	0/7
Group E	8	7/8	2/8 (<5)	0/8

See also Figure 5.

(IACUC protocols used CHLA 353 and St. Jude 558). Non-tumor-bearing naive *Es1*^{e}/SCID mice, both male and female, 8–12 weeks old, were intravenously injected with hCE1m6-NSCs (2×10^6 cells/200 μl), pre-labeled with Feraheme (FE) as previously described.[42] Mice were euthanized 1 hr, 24 hr, 48 hr, or 5 days after hCE1m6-NSC administration. Mouse tissues (lung, liver, spleen, brain, and blood) were snap frozen, and genomic DNA was isolated for TaqMan qPCR analysis to identify the presence of NSCs. The primer sequences and probe were designed to target gag-v-*myc* that is unique to our NSC line.[19,20] The limit of detection is two copies of v-*myc* per 1 μg starting DNA. The limit of quantitation (i.e., the lowest standard) is eight copies per 1 μg of tissue. Note that these NSCs contain one copy of v-*myc* per cell.[41] GAPDH was also quantified as an internal control gene by using real-time qPCR with SYBR Green Supermix (Bio-Rad) for DNA from mouse tissues. Lung, liver, brain, and whole-blood samples were analyzed by qPCR for the presence of v-*myc* to detect NSCs over time. Each organ was divided into one to three pieces for PCR analysis, depending on the starting size of the tissue, and each tissue sample was run in triplicate on a 96-well plate.

Statistical Analyses

Averages were compared using analysis of variance with Bonferroni adjustment for pairwise comparisons of other organs to lung (GraphPad Prism version 6).

NSC Biodistribution Studies in Subcutaneous NB Tumors

Subcutaneous xenograft models of CHLA-255 and CHLA-136 Ffluc-labeled human NB tumors (5×10^6 cells) were established in 6- to 12-week-old male and female *Es1*^{e}/SCID mice (n = 5 per NB type) to determine the biodistribution of intravenously administered hCE1m6-NSCs at the tumor site. All mice were pre-treated with rat anti-mouse CD122 antibody (200 μg/mouse, injected intraperitoneally)[43] and total body irradiation at 200 cGy before NB cell injection. Tumor development was monitored weekly by Xenogen imaging and visual examination. Once tumors were detectable (generally 2–3 weeks after NB cell injection), all mice were intravenously injected with hCE1m6-NSCs (2×10^6 cells/200 μl PBS). Mice were sacrificed on 2 days after NSC injections. Tumor tissues were snap frozen and genomic DNA was isolated for qPCR analysis to identify the presence of NSCs. Each tumor was divided into four quarters, DNA was isolated from each quarter, and two to four DNA samples per tumor were analyzed for v-*myc* using qPCR as described above. Averages were compared using ANOVA with Bonferroni correction for pairwise comparisons (GraphPad Prism version 6).

hCE1m6-NSC and Irinotecan Pharmacokinetic Studies

Subcutaneous NB tumors were established as described above. When tumors became palpable (~5 mm in diameter), mice were intravenously injected with hCE1m6-NSCs (2×10^6 cells), followed 2 days later by intravenous irinotecan injections (15 mg/kg). Mice were euthanized 1 hr after irinotecan injections. One to six replicate measurements of drug concentrations were taken in each mouse, and the maximum concentration was used for analyses. SN-38 concentrations are reported as means ± SD. Fold differences in concentrations by NSC administration were reported, and averages were compared using unpaired t tests (GraphPad Prism version 6).

hCE1m6-NSC and Irinotecan Therapeutic Efficacy Studies in Mice Bearing Metastatic NB

Adult *Es1*^{e}/SCID mice, 6–12 weeks old, both male and female, were used in all experiments. Eight mice per group were injected intravenously with 2×10^6 NB cells (CHLA-136, CHLA-255) on day 0. Two days after administration of hCE1m6-NSCs (2×10^6 NSCs were intravenously administered to mice on day 10 after NB cell injection), mice were treated with three rounds of irinotecan using an established clinical dosing regimen. Treatment groups included: group A, tumor only; group B, irinotecan only (7.5 mg/kg, three times a week); group C, hCE1m6-NSCs + irinotecan (7.5 mg/kg, three times a week); group D, irinotecan only (15 mg/kg, three times a week); and group E, hCE1m6-NSCs + irinotecan (15 mg/kg, three times a week). Two weeks of treatment was followed by 1 week of rest (considered one cycle of therapy). The treatment cycle was repeated three to four times. Tumor growth was monitored by bioluminescent imaging: mean signal intensities were obtained from scans at multiple time points for each mouse. Results were analyzed using random intercept and slope regression models with intensities analyzed on a log scale. Models included quadratic time, group, and their interactions. Significant estimated group differences from curves were analyzed using t tests. t tests on raw data were used to confirm earliest time point of difference. Estimated differences from model curves are reported here. Kaplan-Meier curves were created and median survival with 95% confidence intervals were estimated. Survival curves among cell lines were compared using log-rank test. Pairwise comparisons were made with Sidak for multiple comparisons. Kaplan-Meier survival curves and regression models were analyzed in SAS version 9.4.

AUTHOR CONTRIBUTIONS

M.G., A.J.A., T.W.S., R.S., C.A., R.A.M., and P.M.P. designed the experiments, analyzed data, and drafted and finalized manuscript. L.G. assisted with experimental design and conducted all biostatistical analysis. R.S. and P.M.P. developed the animal models. R.S. and C.A. contributed to the clinical relevance of the experiments. M.M., A.H., L.S.T., R.T., L.T., and Z.W. developed protocols and conducted in vitro and in vivo experiments, acquired data, analyzed data, and created figures. K.S.A., R.A.M., and P.M.P. oversaw all aspects of

the studies and analysis. All authors were involved in critical review of the manuscript.

CONFLICTS OF INTEREST

K.S.A. and A.J.A. are uncompensated board members, officers, and shareholders of TheraBiologics, Inc.

ACKNOWLEDGMENTS

The authors acknowledge the editorial assistance of Dr. Keely L. Walker and citation support of Andrea Lynch (City of Hope). We are grateful to Shu Mi for qualifying and running the v-*myc* and RCR qPCR assays. This research was supported by grants from the NIH-NINDS cooperative program in translational research of the NIH (1-U01-NS082328-01), the Arthur and Rosalinde Gilbert Foundation, the NIH-NCI Cancer Center (core grant P30-CA21765), the American Lebanese Syrian Associated Charities (ALSAC), St. Jude Children's Research Hospital (SJCRH), and City of Hope. Additionally, research reported in this publication included work performed in the following City of Hope core facilities, which are supported by the NCI under award number P30-CA33572: Analytical Pharmacology, Pathology, and Biostatistics. The content in this manuscript is solely the responsibility of the authors and does not necessarily represent the official view of the NIH.

REFERENCES

1. Matthay, K.K. (1997). Neuroblastoma: biology and therapy. Oncology (Williston Park) 11: 1857–1866; discussion 1869–1872, 1875.
2. Seeger, R.C., Brodeur, G.M., Sather, H., Dalton, A., Siegel, S.E., Wong, K.Y., and Hammond, D. (1985). Association of multiple copies of the N-myc oncogene with rapid progression of neuroblastomas. N. Engl. J. Med. *313*, 1111–1116.
3. Shimada, H., Stram, D.O., Chatten, J., Joshi, V.V., Hachitanda, Y., Brodeur, G.M., Lukens, J.N., Matthay, K.K., and Seeger, R.C. (1995). Identification of subsets of neuroblastomas by combined histopathologic and N-myc analysis. J. Natl. Cancer Inst. *87*, 1470–1476.
4. London, W.B., Castleberry, R.P., Matthay, K.K., Look, A.T., Seeger, R.C., Shimada, H., Thorner, P., Brodeur, G., Maris, J.M., Reynolds, C.P., and Cohn, S.L. (2005). Evidence for an age cutoff greater than 365 days for neuroblastoma risk group stratification in the Children's Oncology Group. J. Clin. Oncol. *23*, 6459–6465.
5. Schmidt, M.L., Lal, A., Seeger, R.C., Maris, J.M., Shimada, H., O'Leary, M., Gerbing, R.B., and Matthay, K.K. (2005). Favorable prognosis for patients 12 to 18 months of age with stage 4 nonamplified MYCN neuroblastoma: a Children's Cancer Group Study. J. Clin. Oncol. *23*, 6474–6480.
6. Matthay, K.K., Villablanca, J.G., Seeger, R.C., Stram, D.O., Harris, R.E., Ramsay, N.K., Swift, P., Shimada, H., Black, C.T., Brodeur, G.M., et al.; Children's Cancer Group (1999). Treatment of high-risk neuroblastoma with intensive chemotherapy, radiotherapy, autologous bone marrow transplantation, and 13-cis-retinoic acid. N. Engl. J. Med. *341*, 1165–1173.
7. Berthold, F., Boos, J., Burdach, S., Erttmann, R., Henze, G., Hermann, J., Klingebiel, T., Kremens, B., Schilling, F.H., Schrappe, M., et al. (2005). Myeloablative megatherapy with autologous stem-cell rescue versus oral maintenance chemotherapy as consolidation treatment in patients with high-risk neuroblastoma: a randomised controlled trial. Lancet Oncol. *6*, 649–658.
8. Matthay, K.K., Atkinson, J.B., Stram, D.O., Selch, M., Reynolds, C.P., and Seeger, R.C. (1993). Patterns of relapse after autologous purged bone marrow transplantation for neuroblastoma: a Childrens Cancer Group pilot study. J. Clin. Oncol. *11*, 2226–2233.
9. Yu, A.L., Gilman, A.L., Ozkaynak, M.F., London, W.B., Kreissman, S.G., Chen, H.X., Smith, M., Anderson, B., Villablanca, J.G., Matthay, K.K., et al.; Children's Oncology Group (2010). Anti-GD2 antibody with GM-CSF, interleukin-2, and isotretinoin for neuroblastoma. N. Engl. J. Med. *363*, 1324–1334.
10. Danks, M.K., Morton, C.L., Krull, E.J., Cheshire, P.J., Richmond, L.B., Naeve, C.W., Pawlik, C.A., Houghton, P.J., and Potter, P.M. (1999). Comparison of activation of CPT-11 by rabbit and human carboxylesterases for use in enzyme/prodrug therapy. Clin. Cancer Res. *5*, 917–924.
11. DuBois, S.G., Marachelian, A., Fox, E., Kudgus, R.A., Reid, J.M., Groshen, S., Malvar, J., Bagatell, R., Wagner, L., Maris, J.M., et al. (2016). Phase I study of the Aurora A kinase inhibitor alisertib in combination with irinotecan and temozolomide for patients with relapsed or refractory neuroblastoma: a NANT (New Approaches to Neuroblastoma Therapy) Trial. J. Clin. Oncol. *34*, 1368–1375.
12. Buhl, I.K., Gerster, S., Delorenzi, M., Jensen, T., Jensen, P.B., Bosman, F., Tejpar, S., Roth, A., Brunner, N., Hansen, A., and Knudsen, S. (2016). Cell line derived 5-FU and irinotecan drug-sensitivity profiles evaluated in adjuvant colon cancer trial data. PLoS ONE *11*, e0155123.
13. Chen, M.C., Lee, N.H., Hsu, H.H., Ho, T.J., Tu, C.C., Chen, R.J., Lin, Y.M., Viswanadha, V.P., Kuo, W.W., and Huang, C.Y. (2016). Inhibition of NF-kappaB and metastasis in irinotecan (CPT-11)-resistant LoVo colon cancer cells by thymoquinone via JNK and p38. Environ. Toxicol., Published online April 5, 2016. http://dx.doi.org/10.1002/tox.22268.
14. Wagner, L.M. (2015). Fifteen years of irinotecan therapy for pediatric sarcoma: where to next? Clin. Sarcoma Res. *5*, 20.
15. Kurucu, N., Sari, N., and Ilhan, I.E. (2015). Irinotecan and temozolamide treatment for relapsed Ewing sarcoma: a single-center experience and review of the literature. Pediatr. Hematol. Oncol. *32*, 50–59.
16. Verschraegen, C.F., Movva, S., Ji, Y., Schmit, B., Quinn, R.H., Liem, B., Bocklage, T., and Shaheen, M. (2013). A phase I study of the combination of temsirolimus with irinotecan for metastatic sarcoma. Cancers (Basel) *5*, 418–429.
17. Nogami, N., Hotta, K., Segawa, Y., Takigawa, N., Hosokawa, S., Oze, I., Fujii, M., Ichihara, E., Shibayama, T., Tada, A., et al. (2012). Phase II study of irinotecan and amrubicin in patients with relapsed non-small cell lung cancer: Okayama Lung Cancer Study Group Trial 0402. Acta Oncol. *51*, 768–773.
18. Akie, K., Oizumi, S., Ogura, S., Shinagawa, N., Kikuchi, E., Fukumoto, S., Harada, M., Kinoshita, I., Kojima, T., Harada, T., et al.; Hokkaido Lung Cancer Clinical Study Group (2011). Phase II study of irinotecan plus S-1 combination for previously untreated advanced non-small cell lung cancer: Hokkaido Lung Cancer Clinical Study Group Trial (HOT) 0601. Oncology *81*, 84–90.
19. Zhao, D., Najbauer, J., Annala, A.J., Garcia, E., Metz, M.Z., Gutova, M., Polewski, M.D., Gilchrist, M., Glackin, C.A., Kim, S.U., and Aboody, K.S. (2012). Human neural stem cell tropism to metastatic breast cancer. Stem Cells *30*, 314–325.
20. Yi, B.R., Kim, S.U., and Choi, K.C. (2016). Synergistic effect of therapeutic stem cells expressing cytosine deaminase and interferon-beta via apoptotic pathway in the metastatic mouse model of breast cancer. Oncotarget *7*, 5985–5999.
21. Yang, J., Lam, D.H., Goh, S.S., Lee, E.X., Zhao, Y., Tay, F.C., Chen, C., Du, S., Balasundaram, G., Shahbazi, M., et al. (2012). Tumor tropism of intravenously injected human-induced pluripotent stem cell-derived neural stem cells and their gene therapy application in a metastatic breast cancer model. Stem Cells *30*, 1021–1029.
22. Kim, K.Y., Kim, S.U., Leung, P.C., Jeung, E.B., and Choi, K.C. (2010). Influence of the prodrugs 5-fluorocytosine and CPT-11 on ovarian cancer cells using genetically engineered stem cells: tumor-tropic potential and inhibition of ovarian cancer cell growth. Cancer Sci. *101*, 955–962.
23. Yi, B.R., Kim, S.U., and Choi, K.C. (2014). Co-treatment with therapeutic neural stem cells expressing carboxyl esterase and CPT-11 inhibit growth of primary and metastatic lung cancers in mice. Oncotarget *5*, 12835–12848.
24. Aboody, K.S., Najbauer, J., and Danks, M.K. (2008). Stem and progenitor cell-mediated tumor selective gene therapy. Gene Ther. *15*, 739–752.
25. Dickson, P.V., Hamner, J.B., Burger, R.A., Garcia, E., Ouma, A.A., Kim, S.U., Ng, C.Y., Gray, J.T., Aboody, K.S., Danks, M.K., and Davidoff, A.M. (2007). Intravascular administration of tumor tropic neural progenitor cells permits targeted delivery of interferon-beta and restricts tumor growth in a murine model of disseminated neuroblastoma. J. Pediatr. Surg. *42*, 48–53.
26. Sims, T.L., Jr., Hamner, J.B., Bush, R.A., Fischer, P.E., Kim, S.U., Aboody, K.S., McCarville, B., Danks, M.K., and Davidoff, A.M. (2009). Neural progenitor cell-mediated delivery of osteoprotegerin limits disease progression in a preclinical

model of neuroblastoma bone metastasis. J. Pediatr. Surg. *44*, 204–210, discussion 210–211.

27. Aboody, K.S., Najbauer, J., Metz, M.Z., D'Apuzzo, M., Gutova, M., Annala, A.J., Synold, T.W., Couture, L.A., Blanchard, S., Moats, R.A., et al. (2013). Neural stem cell-mediated enzyme/prodrug therapy for glioma: preclinical studies. Sci. Transl. Med. *5*, 184ra59.

28. Aboody, K.S., Najbauer, J., Schmidt, N.O., Yang, W., Wu, J.K., Zhuge, Y., Przylecki, W., Carroll, R., Black, P.M., and Perides, G. (2006). Targeting of melanoma brain metastases using engineered neural stem/progenitor cells. Neuro-oncol. *8*, 119–126.

29. Gutova, M., Shackleford, G.M., Khankaldyyan, V., Herrmann, K.A., Shi, X.H., Mittelholtz, K., Abramyants, Y., Blanchard, M.S., Kim, S.U., Annala, A.J., et al. (2013). Neural stem cell-mediated CE/CPT-11 enzyme/prodrug therapy in transgenic mouse model of intracerebellar medulloblastoma. Gene Ther. *20*, 143–150.

30. Aboody, K.S., Bush, R.A., Garcia, E., Metz, M.Z., Najbauer, J., Justus, K.A., Phelps, D.A., Remack, J.S., Yoon, K.J., Gillespie, S., et al. (2006). Development of a tumor-selective approach to treat metastatic cancer. PLoS ONE *1*, e23.

31. Portnow, J., Synold, T.W., Badie, B., Tirughana, R., Lacey, S.F., D'Apuzzo, M., Metz, M.Z., Najbauer, J., Bedell, V., Vo, T., et al. (2016). Neural stem cell-based anti-cancer gene therapy: a first-in-human study in recurrent high grade glioma patients. Clin Cancer Res., Published online December 15, 2016. http://dx.doi.org/10.1158/1078-0432.CCR-16-1518.

32. Wierdl, M., Tsurkan, L., Hyatt, J.L., Edwards, C.C., Hatfield, M.J., Morton, C.L., Houghton, P.J., Danks, M.K., Redinbo, M.R., and Potter, P.M. (2008). An improved human carboxylesterase for enzyme/prodrug therapy with CPT-11. Cancer Gene Ther. *15*, 183–192.

33. Metz, M.Z., Gutova, M., Lacey, S.F., Abramyants, Y., Vo, T., Gilchrist, M., Tirughana, R., Ghoda, L.Y., Barish, M.E., Brown, C.E., et al. (2013). Neural stem cell-mediated delivery of irinotecan-activating carboxylesterases to glioma: implications for clinical use. Stem Cells Transl. Med. *2*, 983–992.

34. Patterson, A.V., Saunders, M.P., and Greco, O. (2003). Prodrugs in genetic chemoradiotherapy. Curr. Pharm. Des. *9*, 2131–2154.

35. Oosterhoff, D., Pinedo, H.M., van der Meulen, I.H., de Graaf, M., Sone, T., Kruyt, F.A., van Beusechem, V.W., Haisma, H.J., and Gerritsen, W.R. (2002). Secreted and tumour targeted human carboxylesterase for activation of irinotecan. Br. J. Cancer *87*, 659–664.

36. Morton, C.L., Iacono, L., Hyatt, J.L., Taylor, K.R., Cheshire, P.J., Houghton, P.J., Danks, M.K., Stewart, C.F., and Potter, P.M. (2005). Activation and antitumor activity of CPT-11 in plasma esterase-deficient mice. Cancer Chemother. Pharmacol. *56*, 629–636.

37. Fischer, U.M., Harting, M.T., Jimenez, F., Monzon-Posadas, W.O., Xue, H., Savitz, S.I., Laine, G.A., and Cox, C.S., Jr. (2009). Pulmonary passage is a major obstacle for intravenous stem cell delivery: the pulmonary first-pass effect. Stem Cells Dev. *18*, 683–692.

38. Kushner, B.H., Modak, S., Kramer, K., Basu, E.M., Roberts, S.S., and Cheung, N.K. (2013). 5-day/5-drug myeloablative outpatient regimen for resistant neuroblastoma. Bone Marrow Transplant. *48*, 642–645.

39. Morshed, R.A., Gutova, M., Juliano, J., Barish, M.E., Hawkins-Daarud, A., Oganesyan, D., Vazgen, K., Yang, T., Annala, A., Ahmed, A.U., et al. (2015). Analysis of glioblastoma tumor coverage by oncolytic virus-loaded neural stem cells using MRI-based tracking and histological reconstruction. Cancer Gene Ther. *22*, 55–61.

40. Liu, Y., Wu, H.W., Sheard, M.A., Sposto, R., Somanchi, S.S., Cooper, L.J., Lee, D.A., and Seeger, R.C. (2013). Growth and activation of natural killer cells ex vivo from children with neuroblastoma for adoptive cell therapy. Clin. Cancer Res. *19*, 2132–2143.

41. Danks, M.K., Yoon, K.J., Bush, R.A., Remack, J.S., Wierdl, M., Tsurkan, L., Kim, S.U., Garcia, E., Metz, M.Z., Najbauer, J., et al. (2007). Tumor-targeted enzyme/prodrug therapy mediates long-term disease-free survival of mice bearing disseminated neuroblastoma. Cancer Res. *67*, 22–25.

42. Gutova, M., Frank, J.A., D'Apuzzo, M., Khankaldyyan, V., Gilchrist, M.M., Annala, A.J., Metz, M.Z., Abramyants, Y., Herrmann, K.A., Ghoda, L.Y., et al. (2013). Magnetic resonance imaging tracking of ferumoxytol-labeled human neural stem cells: studies leading to clinical use. Stem Cells Transl. Med. *2*, 766–775.

43. Xu, Y., Sun, J., Sheard, M.A., Tran, H.C., Wan, Z., Liu, W.Y., Asgharzadeh, S., Sposto, R., Wu, H.W., and Seeger, R.C. (2013). Lenalidomide overcomes suppression of human natural killer cell anti-tumor functions by neuroblastoma microenvironment-associated IL-6 and TGFβ1. Cancer Immunol. Immunother. *62*, 1637–1648.